available at www.sciencedirect.com

ScienceDirect

journal homepage: www.elsevier.com/locate/ijrefrig

Water-coupled carbon dioxide microchannel gas cooler for heat pump water heaters: Part II – Model development and validation

*Brian M. Fronk, Srinivas Garimella**

Sustainable Thermal Systems Laboratory, George W. Woodruff School of Mechanical Engineering, Georgia Institute of Technology, Atlanta, GA 30332, USA

ARTICLE INFO

Article history:
Received 15 January 2010
Received in revised form
19 April 2010
Accepted 19 May 2010
Available online 8 June 2010

Keywords:
Heat exchanger
Gas cooler
Carbon dioxide
Transcritical cycle
Microchannel
Heat pump
Heating
Hot water
Modelling
Simulation

ABSTRACT

An experimental and analytical study on the performance of a compact, microchannel water-carbon dioxide (CO_2) gas cooler was conducted. The experimental results addressed in Part I of this study are used here in Part II to develop an analytical model, utilizing a segmented approach to account for the steep gradients in the thermodynamic and transport properties of supercritical CO_2. The model predicted gas cooler heat duty with an average absolute deviation of 7.5% with varying refrigerant and water inlet conditions. The segmented model reveals that near the pseudo-critical point, there is a significant local decrease in refrigerant-side thermal resistance, which yields a sharp increase in local heat duty. The impact of this spike on gas cooler performance is analyzed. Results from this study can be used to predict the effect of changing geometric parameters of the heat exchanger without the need for expensive prototype development and testing.

Refroidisseur de gaz à microcanaux sur eau souterraine pour des pompes à chaleur au dioxyde de carbone utilisées pour chauffer de l'eau sanitaire : Partie II – Développement et validation du modèle

Mots clés : échangeur de chaleur ; refroidisseur de gaz ; dioxyde de carbone ; cycle transcritique ; micro-canal ; pompe à chaleur ; chauffage ; eau sanitaire ; modélisation - simulation

* *Corresponding author.*
E-mail address: sgarimella@gatech.edu (S. Garimella).
0140-7007/$ – see front matter © 2010 Elsevier Ltd and IIR. All rights reserved.
doi:10.1016/j.ijrefrig.2010.05.012

Nomenclature

A	heat transfer area (m^2)
A_c	fin flow area (m^2)
C_{min}	minimum thermal capacitance rate (kW K^{-1})
D	tube diameter (m)
D_h	fin hydraulic diameter (m)
G	mass flux (kg m^{-2} s^{-1})
f	friction factor (–)
h	heat transfer coefficient (kW m^{-2} K^{-1})
j	colburn factor (–)
L	length (m)
l	fin length (m)
$\dot{m}$	mass flow rate (g s^{-1})
Nu	Nusselt number (–)
P	pressure (kPa)
Pr	Prandtl number (–)
$\dot{Q}$	heat duty (kW)
R	thermal resistance (K kW^{-1})
Re	Reynolds number (–)
T	temperature (°C)

Greek symbols

α	fin geometric parameter (–)
β	fin geometric parameter (–)
δ	fin geometric parameter (–)
ε	Effectiveness (–)
ρ	Density (kg m^{-3})

Subscripts

b	bulk
eff	effective
ref	refrigerant-side
seg	local segment

1. Introduction

A desire to utilize more environmentally friendly refrigerants has spurred interest in the development of vapor compression systems with carbon dioxide (CO_2) as the working fluid. CO_2 has a low global warming potential (GWP = 1), favorable transport properties, low cost, high availability, and is nonflammable and non-toxic. Unlike conventional refrigerants, CO_2 has a relatively low critical temperature and pressure (31.1 °C/73.7 bar). Therefore, under most conditions of interest, the system operates as a transcritical cycle. Rather than a constant temperature condensation process, the supercritical CO_2 exhibits a temperature glide through the component known as the gas cooler.

One of the most promising applications of CO_2 heat pump devices is the provision of domestic hot water, either as a stand-alone water heater, or in conjunction with a chiller function. The high temperature lifts required in water heating match well with the temperature glide exhibited by the supercritical CO_2. The glide allows water delivery temperatures of up to 90 °C without significant degradation in system efficiency (Kim et al., 2004). Attempting to heat water to this temperature with a conventional system (e. g., R134a) could only be accomplished by raising the compressor discharge pressure to a high magnitude to eliminate temperature pinches. In doing so, the available enthalpy difference across the vapor-liquid dome decreases, and the compressor pressure ratio increases, drastically reducing system efficiency.

In addition to the temperature glide, CO_2 thermodynamic and transport properties vary significantly in the region near the critical point. These variations have a significant impact on local heat transfer and must be accounted for. Due to these property variations, analyzing the gas cooler through an overall log mean temperature difference (LMTD) or effectiveness-NTU method yields only approximate estimates, and a segmented approach must be utilized to achieve accurate performance predictions.

A method of evaluating the supercritical CO_2 heat transfer coefficient is required to develop gas cooler models of reasonable accuracy. Cheng et al. (2008) present an extensive review of supercritical CO_2 correlations for heat transfer coefficient and friction factor in macro and microchannels. Based on the experimental results of several researchers, they conclude that there is no consensus for a best correlation for predicting heat transfer and pressure drop, absent further experimental data. Many authors (Yin et al., 2001; Cecchinato et al., 2005; Hwang et al., 2005) have predicted the heat transfer coefficient of supercritical CO_2 using a constant property, single-phase model such as the Gnielinski (1976) correlation. The Gnielinski correlation is valid for turbulent flows with $2300 < Re < 5 \times 10^6$ and $0.5 < Pr < 2000$. For supercritical flows, this correlation has been shown to under predict the heat transfer coefficient, particularly near the pseudo-critical temperature (Wang and Hihara, 2002). At low Re near the critical point and in heated upward flow, the property differences between the wall and bulk fluid become significant (Pettersen et al., 1998). Other correlations account for these effects. In a critical review of supercritical CO_2 heat transfer coefficients, Pitla et al. (1998) discuss the correlation developed by Krasnoshchekov et al. (1970) for supercritical gas cooling in horizontal tubes. This correlation addresses the effects of the difference between bulk and wall temperatures on the heat transfer coefficient. When the tube wall temperature is below the critical temperature of the fluid, the predicted heat transfer coefficient using the property corrections is seen to increase compared to that of a constant property single-phase fluid. An experimental investigation of supercritical CO_2 cooling by Baskov et al. (1977) found the effect of free convection to be negligible at high Re. They proposed a correlation for cooling of supercritical CO_2 in vertical tubes. Pitla et al. (1998) compared the Krasnoshchekov et al. (1970); Baskov et al. (1977), and a numerically derived correlation proposed by Petrov and Popov (1985) with the correlation by Petukhov and Kirillov (1958). The correlations were plotted at a mass flow rate of 30 g s^{-1}, pressure of 100 bar, refrigerant temperature of 32–120 °C and a heat sink temperature of 17–32 °C. The tube under consideration had an ID of 4.572 mm and an OD of 6.35 mm. The authors show that throughout the

range of carbon dioxide temperatures, the Baskov et al. (1977) and Petrov and Popov (1985) correlations are in good agreement. The Krasnoshchekov et al. (1970) correlation is in good agreement when the carbon dioxide temperature is outside the pseudo-critical range.

Many researchers have modeled the performance of water- and air-coupled gas coolers for use in split-system AC/heat pumps, mobile air conditioning systems and water heating systems using a variety of heat transfer and pressure drop correlations. A majority of the modeling studies are utilized in system level models for simulating overall performance. Most researchers employ a finite volume approach to account for the changing supercritical CO_2 properties, particularly near the pseudo-critical point. A brief overview of modeling techniques and comparisons with experimental data is provided here. Yin et al. (2001) developed a segmented model of an air-coupled, parallel-serpentine gas cooler consisting of three passes of 13, 11 and 10 microchannel tubes with louvered fins. There were 11 circular ports per tube with ID = 0.79 mm. Refrigerant heat transfer coefficient in each segment was calculated from the Gnielinski (1976) correlation and pressure drop from the Churchill (1977) correlation. Conduction between tubes was neglected, and the incoming air was assumed to have uniform velocity and temperature. Local heat duty in each segment was calculated based on the log mean temperature difference (LMTD) method. The simulation model was validated with 358 data points corresponding to 48 different indoor/outdoor operating conditions. They showed agreement in predicted heat duty within ±2%, while refrigerant pressure drop was systematically under predicted by approximately a factor of 3, which was attributed to potential manufacturing defects in the microchannel tubes. Garimella (2002) presented a model for a near-counter flow air-coupled CO_2 gas cooler using serpentine refrigerant tubes and louvered fins on the air-side. The geometry required the tracking of refrigerant and air temperature along both the length and width of each refrigerant tube. The simulated gas cooler had 36 tubes with six 1.905 mm diameter circular ports per tube. The effectiveness-NTU method was employed to obtain the local heat duty in each segment. The Krasnoshchekov et al. (1970) correlation was used to predict the local heat transfer coefficient. With a volumetric air flow rate of 0.334 $m^3\ s^{-1}$ and a refrigerant mass flow rate of 31 g s^{-1}, the model predicted a heat duty of 6.97 kW and an approach temperature difference of 5.3 K. Garimella (2003) extended this analysis to include axial conduction losses due to heat transfer between adjacent tubes through the louvered fins, and demonstrated a reduction in heat duty of 13% at an unlouvered fin fraction of 30%. Ortiz et al. (2003) developed and incorporated a segmented model of an air-coupled microchannel gas cooler into a split-system simulation model. The gas cooler was a cross flow, extruded aluminum design. The heat duty in each segment is solved in iterative fashion, where an initial tube wall temperature is estimated, and then heat duty found from the effectiveness-NTU method and from evaluating the local $UA\times\Delta T$. Refrigerant heat transfer coefficient is calculated from the modified Gnielinski correlation (Pettersen et al., 2000) at high mass flux ($G > 350\ kg\ m^{-2}\ s^{-1}$) and the Petrov and Popov (1985) correlation at lower mass fluxes. Refrigerant pressure drop was calculated in each segment using the friction factor correlation of Kuraeva and Protopopov (1974). Additionally, entrance and compressibility effects were considered. The individual model was validated with experimental test data from Zhao et al. (2001), which featured microchannel tubes with ten 1.0 mm diameter ports per tube. The model predicted heat duty within 3% of CO_2-side measurements and 5% of air-side measurements, with poorer agreement at low refrigerant mass fluxes attributed to the potential inapplicability of the modified Gnielinski correlation.

Kim et al. (2005) developed a model of a water-coupled gas cooler for use in a system model for evaluating the performance of a transcritical system with a suction line heat exchanger in water heating applications. The modeled gas cooler was a tube-in-tube counterflow geometry, with refrigerant tube ID = 7.5 mm, and water tube ID = 14.9 mm. The gas cooler was divided into equal length segments, with the local heat duty calculated using the LMTD method. Refrigerant heat transfer coefficient and pressure drop were calculated from the Krasnoshchekov et al. (1970) and Petrov and Popov (1985) correlations. The model was not independently validated; however, they reported that the system model predicted system heat duty with an absolute mean deviation of 3.56%. Cecchinato et al. (2005) developed a similar segmented model of a water-coupled, tube-in-tube gas cooler for use in a system model. The simulated refrigerant tube had an ID = 6.5 mm and the outer water tube ID varied from 15.0 to 30.1 mm, depending on test condition. Simulations were carried out comparing CO_2 transcritical cycle performance to R134a performance for different operating conditions. No experimental validation was presented in the study. Sarkar et al. (2006) reported a gas cooler component model that was part of a larger system model for predicting transcritical cycle performance in simultaneous water heating and cooling operations. Again, the gas cooler under consideration was a water-coupled counterflow tube-in-tube heat exchanger, with an inner tube OD of 6.35 mm and thickness of 0.8 mm, outer tube OD of 12 mm and thickness of 1 mm. The model was discretized and local heat duty found from the LMTD method. The correlation proposed by Pitla et al. (2002) for refrigerant-side heat transfer coefficient and the Petrov and Popov (1985) equation for friction factor were used. The gas cooler model was not individually validated using component-level measurements; however, the overall system model showed agreement with a 15% maximum deviation in predicted COP, with poorest agreement at low compressor discharge pressure (<80 bar) in data presented by Sarkar et al. (2009).

Chang and Kim (2007) developed a simulation model of an air-coupled gas cooler consisting of two or three banks of serpentine tubes connected in series. Each bank consisted of between eight and twelve 7 mm OD microfin tubes with louvered fins. The heat exchanger under investigation was a multi-pass cross flow configuration. They treated each tube in each bank as a cross flow heat exchanger, and assumed a constant CO_2 heat transfer coefficient based on the single-phase correlation of Han and Lee (2005) for microfin tubes. The correlation was developed from data on water for tubes with an OD from 5.1 to 9.52 mm. They theorized that since the air-side resistance dominated heat transfer, uncertainties in the

refrigerant-side would have a negligible effect on heat exchanger performance. At a refrigerant mass flow rate of 70 g s^{-1}, the predicted heat duty varied from 2 to 4 kW, with variations from experimental data within ±10%. Koyama et al. (2009) developed a model of an air-coupled cross-counter flow fin-tube heat exchanger. The ID of the simulated refrigerant tubes was 4.75 mm. The heat exchanger was divided into $i \times j \times k$ segments to account for varying refrigerant and air properties and temperature. Each segment was treated as a cross flow heat exchanger, where the local heat duty was calculated as a function of the segment UA and average refrigerant and air temperature difference. The refrigerant heat transfer coefficient was determined from the Dang and Hihara (2004) correlation for supercritical CO_2 and the friction factor from the Blasius equation. The component model was incorporated into a system simulation model. The system model was compared qualitatively with CO_2 refrigeration systems, however no explicit validation of the gas cooler component model was conducted.

Many researchers have employed a segmented approach to modeling CO_2 gas coolers using various correlations for predicting heat transfer coefficient and friction factor. Much of the work has focused on cross flow and near-counter flow air-coupled gas coolers, and relatively simple tube-in-tube counterflow water-coupled heat exchangers. There has been comparatively less work on compact microchannel based CO_2-water gas coolers. The thermal resistance of the water-side of a CO_2-water gas cooler will be much less than that of the air-side in an air-coupled heat exchanger. Thus, accurate prediction of the heat transfer performance of the CO_2 side assumes much greater importance. Generally, investigators have modeled the CO_2-water gas cooler as a simple tube-in-tube geometry for use in cycle simulation models (Cecchinato et al., 2005; Kim et al., 2005; Sarkar et al., 2006; Laipradit et al., 2008). While adequate for system modeling, a tube-in-tube heat exchanger is not an optimized geometry for an actual water heating system. A compact, counterflow gas cooler is the key enabling component to minimize heat exchanger material use and system footprint, while taking advantage of the unique water heating capabilities of transcritical cycles.

In the present work, therefore, an analysis of the heat transfer mechanisms of a water-coupled gas cooler with a compact, multi-pass cross-counter flow design is conducted. A segmented model for an aluminum brazed plate, microchannel CO_2 gas cooler is developed, validated with experimental data presented in companion paper Part I, and used to parametrically evaluate the impacts of changing inlet water and refrigerant conditions. The gas cooler is a multi-pass cross-counterflow, water-coupled heat exchanger intended for heating water. The heat exchanger is composed of several finned plates that function as water passes and multiple microchannel refrigerant tubes. Five-, seven- and a simulated twelve-plate heat exchanger constructed by connecting the two in series were tested and modeled.

2. Model development

A segmented model of a water-coupled CO_2 gas cooler was developed using the Engineering Equation Solver (EES) (Klein, 2008) platform. The model was then validated with data from a water-coupled CO_2 heat pump test facility presented in Part I.

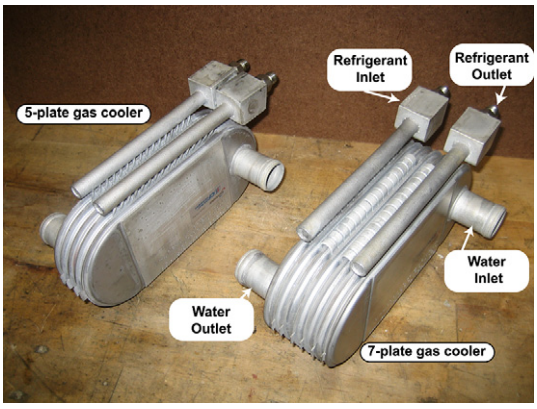

Fig. 1 – Gas cooler photograph.

Fig. 1 shows a photograph and Fig. 2 a cross-sectional schematic of the gas cooler under investigation. Water enters through one side of the heat exchanger and makes several serpentine passes before exiting the heat exchanger. The water channels contain offset strip fins to enhance heat transfer and provide structural stability. Refrigerant enters the inlet header as shown, is divided between 16 refrigerant tubes (each containing four 0.89 mm diameter circular channels), and serpentines between each water channel before exiting on the same side as the water inlet. Thus, the fluid motion is generally counterflow, although the local heat transfer occurs in a cross flow configuration. Table 1 shows the primary dimensions of a seven-plate gas cooler, which is defined as a gas cooler with seven water passes and six refrigerant passes.

The heat exchanger was modeled using a segmented element approach, in which the water passage and the refrigerant tubes were divided into equal sized nodes. A schematic representation of the nodes is shown in Fig. 3. Refrigerant nodes are shaded. Each node transfers heat with

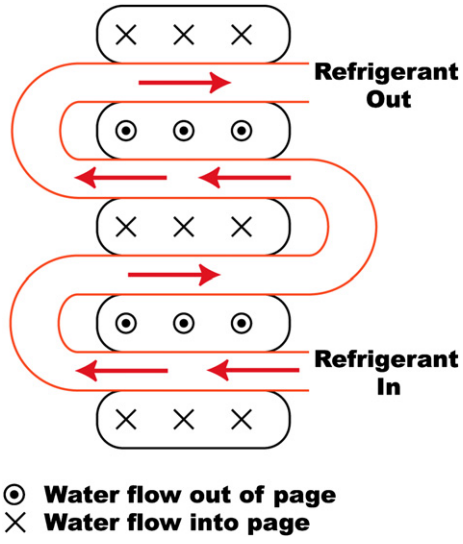

Fig. 2 – Gas cooler cross section schematic.

Table 1 – Seven-plate gas cooler dimensions.

Overall dimensions	
Number of refrigerant tubes	16
Number of water passes	7
Gas cooler length	191 mm
Gas cooler width	54.0 mm
Gas cooler height	84.0 mm
Refrigerant side	
Total refrigerant tube length	516 mm
Refrigerant pass tube length	81.0 mm
Number of channels per tube	4
Channel diameter	0.89 mm
Tube width	6.35 mm
Tube height	1.65 mm
Tube wall thickness	0.38 mm
Tube web thickness	0.64 mm
Refrigerant-side heat transfer area	92,292 mm^2
Water side	
Fin height	6.41 mm
Fin space	2.23 mm
Fin thickness	0.31 mm
Fin length	3.18 mm
Fin pitch	4.4 fins per cm
Water-side heat transfer area	385,140 mm^2

the two neighboring nodes. Water nodes on the two exterior plates were assumed to have an adiabatic boundary on one side. Local heat transfer in each segmented node was solved using the effectiveness-NTU approach for cross flow segments. The resulting system of coupled equations was solved iteratively. The segment length was chosen in a manner in which property variation across the segment was not significant. For a seven-plate gas cooler, 30 segments per tube were used, which yielded less than a 0.4% difference in predicted capacity when compared to a tube with 60 segments.

The local heat duty was calculated using the effectiveness-NTU approach, with NTU based on UA and the minimum thermal capacitance rate, C_{min} of each segment. The local effectiveness was determined as a function of the NTU, assuming that the segment could be approximated as a cross flow heat exchanger with both fluids unmixed. Local heat duty was then determined from Eq. (1), using the water and refrigerant segment inlet temperatures.

$$\dot{Q}_{seg} = \varepsilon \cdot C_{min}\left(T_{ref,in} - T_{water,in}\right) \tag{1}$$

To determine the UA value used in the ε-NTU calculations, the local heat transfer area and heat transfer coefficients, and thermal resistance of the aluminum tube wall were determined. The resulting formulation of UA is shown in Eq. (2). The effective water-side heat transfer coefficient was a function of the local fin efficiency, which was generally predicted to be between 50 and 75%, depending on the water flow rate.

$$UA = \frac{1}{\frac{1}{h_{ref}A_{ref}} + R_w + \frac{1}{h_{water}A_{eff,water}}} \tag{2}$$

The water flow was assumed to be uniform through each segment and fin section. The local heat transfer coefficient was calculated using the Manglik and Bergles correlation (1995) shown in Eq. (4). This correlation was developed for determining the Colburn factor, j, for rectangular offset strip fin geometries such as that utilized in the gas cooler design under consideration. The empirically based correlation considers data in the laminar, transition and turbulent regime, and utilizes an asymptotic matching technique, resulting in one equation valid (Eq. (4)) for all flow regimes. Thus, for the expected water-side Reynolds numbers in the current study ($Re < 1000$), the model is expected to be applicable. The water-side Reynolds number is based on the hydraulic diameter as defined by Manglik and Bergles (1995), shown in Eq. (3).

$$D_h = \frac{4A_c}{A/l} \tag{3}$$

$$j = 0.6522\mathrm{Re}_{water}^{-0.5403}\alpha^{-0.1541}\delta^{0.1499}\gamma^{-0.0678} \times \left[1 + 5.269\times10^{-5}\mathrm{Re}_{water}^{1.340}\alpha^{0.504}\delta^{0.456}\gamma^{-1.055}\right]^{0.1} \tag{4}$$

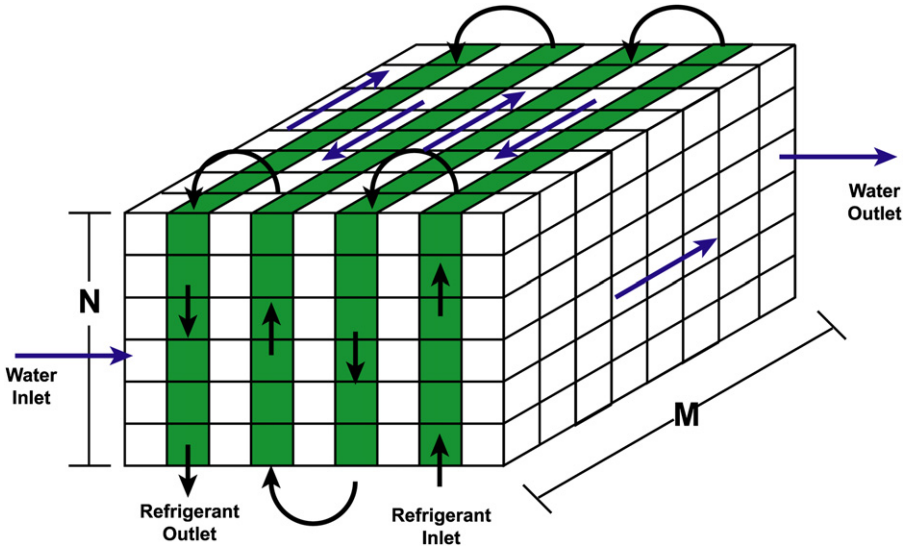

Fig. 3 – Segmented schematic.

The refrigerant-side local heat transfer coefficient was calculated using the Gnielinski (1976) correlation (Eq. (5)), using properties evaluated at the average segment temperature and inlet pressure. The local Fanning friction factor (f) was found using the Filonenko (1954) correlation (Eq. (6)).

$$Nu_D = \frac{(f/8)(Re_D - 1000)Pr_b}{1 + 12.7(f/8)^{1/2}\left(Pr_b^{2/3} - 1\right)} \quad (5)$$

$$f = (0.79 \cdot \ln(Re) - 1.64)^{-2} \quad (6)$$

The refrigerant Reynolds number is based on the local mass flux, viscosity and circular channel diameter. The refrigerant Reynolds numbers under consideration ranged from 3000 to 25,000, which are within the range of applicability of the Gnielinski (1976) correlation. The refrigerant flow is not expected to be purely laminar for any of the mass flow rates investigated. The local refrigerant heat transfer coefficient ranged from 1.5 to over 10 kW m^{-2} K^{-1}, with the peak heat transfer occurring at high mass fluxes in the pseudo-critical region. The local heat duty was used to determine the outlet enthalpy of the water and refrigerant for each segment. The coupled equations were solved simultaneously using the nonlinear solver included with EES.

Refrigerant and water pressure drop predictions were also incorporated into the model. The supercritical CO_2 was treated as a single-phase fluid for calculation of pressure drop as shown in Eq. (7). The friction factor in each segment was calculated using the Churchill (1977) correlation (Darcy version), which is applicable for the laminar, transitional and turbulent regimes. A tube roughness of 5 μm was assumed.

$$\Delta P = \frac{fG^2L}{2\rho D} \quad (7)$$

Minor losses, including microchannel tube bends, entrance effects and exit effects were modeled based on the local flow conditions and the loss coefficient K as presented in White (2003). Most of these coefficients were based on experiments with larger tube diameters, and thus may not be applicable to the geometry of the heat exchanger under investigation.

Water-side pressure drop was calculated using the Fanning friction factor correlation of Manglik and Bergles (1995) shown in Eq. (8), which is a function of the same dimensionless fin geometry parameters used to determine the Colburn factor for heat transfer predictions.

$$f = 9.6243 Re_{water}^{-0.7422} \alpha^{-0.1856} \delta^{0.3053} \gamma^{-0.2659} \times \left[1 + 7.669 \times 10^{-8} Re_{water}^{4.429} \alpha^{0.920} \delta^{3.767} \gamma^{0.236}\right] \quad (8)$$

3. Model validation and analysis

The model described above was validated using experiments on the CO_2 heat pump facility shown schematically in Fig. 4, and described in greater detail in companion paper Part I. Experiments were conducted with a five-, seven- and simulated twelve-plate gas cooler. The twelve-plate gas cooler was formed by connecting the five- and seven-plate gas coolers in series. The gas cooler and evaporator were coupled to separate closed water loops; with the water temperature regulated

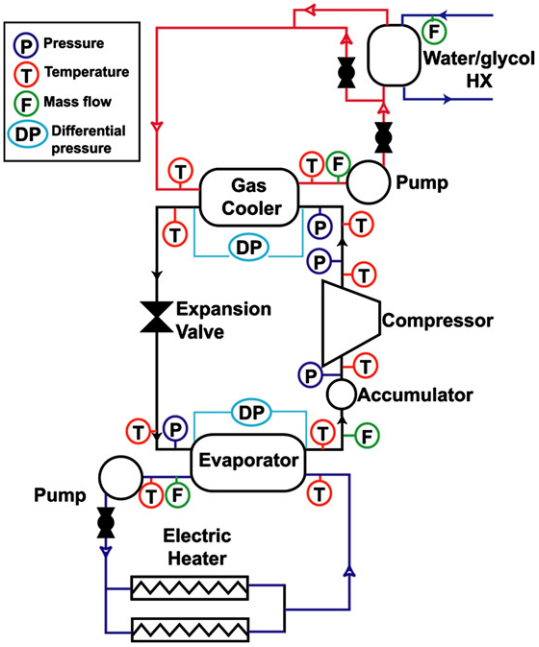

Fig. 4 – Test facility schematic.

using a laboratory chilled water supply and an immersion electric heater bank. Compression was provided by one or two reciprocating compressors, depending on the desired mass flow rate. The compressors were lubricated by a 25 mL charge of polyolester (POE) oil. Thermocouples and pressure transducers at the inlet and outlet of each component allowed the determination of the thermodynamic state. For the gas cooler, the water and refrigerant inlet and outlet enthalpies were determined from the measured temperature and pressure, using the equation of state developed by Span and Wagner (1996) for CO_2. The heat duties for the water and refrigerant sides were determined from the enthalpy difference and the measured mass flow rate of each fluid. The average of the refrigerant- and water-side heat duties was compared with the model predictions.

Over 125 data points were obtained from the three different gas cooler sizes. Experiments were conducted at refrigerant mass flow rates from 8 g s^{-1} to 25 g s^{-1}, with the inlet temperature varying from 85 to 115 °C. High-side pressure ranged from 7900 to 11,000 kPa. The gas cooler water flow rate was varied from 0.93 L min^{-1} to 5.68 L min^{-1}, with inlet temperatures ranging from 5 to 20 °C. Measured heat duties ranged from 2.0 to 6.5 kW, with an uncertainty of ±30 to ±140 W. Further description of the experimental setup and results can be found in companion paper Part I.

The measured gas cooler refrigerant inlet temperature, pressure and mass flow rate, and water inlet temperature and flow rate were used as model inputs for each data point. The predicted heat duty was compared with the measured capacity to validate the model. A plot of predicted versus measured capacity is shown in Fig. 5.

The absolute average difference between measured and predicted heat duty was 7.5%. Agreement was poorest at the lowest water flow rate (0.93 L min^{-1}), with the low water flow rates in the five-plate gas cooler showing the poorest

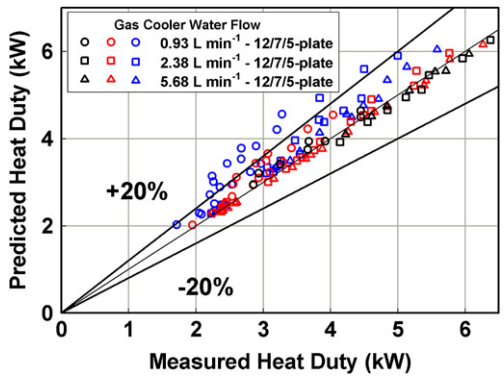

Fig. 5 – Model results.

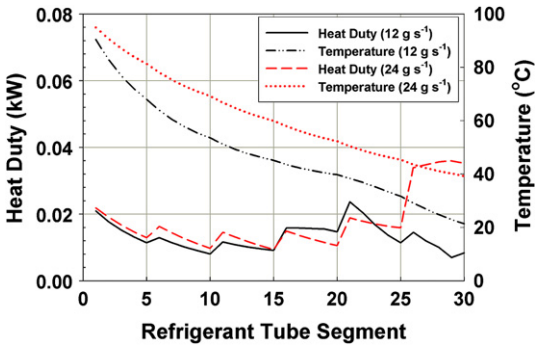

Fig. 6 – Heat duty vs. position.

agreement with the model. Errors at the low water flow rate may be attributed to possible water maldistribution and uncertainty in the water flow rate measurement. Refrigerant pressure drop was systematically under predicted by the model by an average factor of 3.5. This was consistent across all water and refrigerant inlet conditions. This can potentially be attributed to the presence of compressor lubricant, which increases the pressure drop. The ASHRAE standard (2006) for measuring proportion of lubricant in liquid refrigerant calls for a lubricant/refrigerant mixture to be drawn out of the system into an evacuated cylinder of known volume, whereupon the refrigerant is boiled off and the remaining lubricant is weighed. The high operating pressure of the experimental system would require the use of a thick walled cylinder, and require a large volume of refrigerant/lubricant to be removed to resolve the lubricant weight with acceptable accuracy. Due to the small refrigerant charge in the water-coupled system, this was not attempted. However, based on operational experience at Modine (Hoehne, 2007), a lubricant circulation rate of 5% by mass was assumed to explore its effect on pressure drop. The two-phase Lockhart and Martinelli (1949) pressure drop correlation showed some promise in improving the agreement between measured and estimated values with this lubricant mass fraction. However, without accurate measurement of the lubricant circulation rate and an appropriate pressure drop correlation developed for supercritical CO_2 and POE lubricant, accurate pressure drop modeling remains a challenge.

The segmented model, validated with experimental results, can be used as a design tool for predicting gas cooler performance with varying refrigerant and water inlet conditions. The analysis presented here considers a seven-plate gas cooler, with refrigerant inlet temperature varying from 70 to 100 °C, refrigerant flow rates of 12–24 g s^{-1}, refrigerant inlet pressures of 9000–12,000 kPa, water inlet temperatures from 5 to 65 °C and water flow rates of 0.93–5.68 L min^{-1}. The dimensions of the modeled gas cooler are the same as those used in the experimental study, Part I (Table 1).

The segmented model evaluates the local heat transfer coefficient and heat transfer area for the water and refrigerant sides. In a supercritical gas cooler, the properties of the fluid change drastically near the pseudo-critical point as the fluid transitions from a "vapor-like" to "liquid-like" fluid, resulting in an enhanced heat transfer coefficient. In addition to a locally varying heat transfer coefficient, the driving temperature difference between the water and refrigerant varies through the heat exchanger, which results in a large variation in heat duty through the gas cooler. Fig. 6 shows the variation in local heat duty and refrigerant temperature as a function of position for a gas cooler with a water flow rate of 0.93 L min^{-1} and an inlet temperature of 5 °C, and a refrigerant flow rate of 12 and 24 g s^{-1}, with an inlet temperature and pressure of 100 °C and 9000 kPa, respectively. The variation is plotted along a single representative serpentine refrigerant tube (tube 8), which is a good approximation for the trends of the entire heat exchanger.

In Fig. 6, refrigerant segment 1 represents the refrigerant inlet, and segment 30 is the refrigerant outlet. Since the refrigerant/water flow is in a generally counterflow orientation, the temperature of the refrigerant is highest at the inlet, and lowest at the outlet, whereas the water is coolest at the refrigerant outlet and hottest at the refrigerant inlet. In the seven-plate gas cooler, the refrigerant tube makes six passes. These passes are evident in Fig. 6, occurring every five segments. The jump in heat duty between each pass can be attributed to the different water-side boundary conditions of the refrigerant tube in each pass.

The observed spike in heat duty corresponds to the spike in local refrigerant heat transfer coefficient. The spike can be observed between segments 18–22 for the 12 g s^{-1} mass flow and segments 25–30 for the 24 g s^{-1} cases. As the CO_2

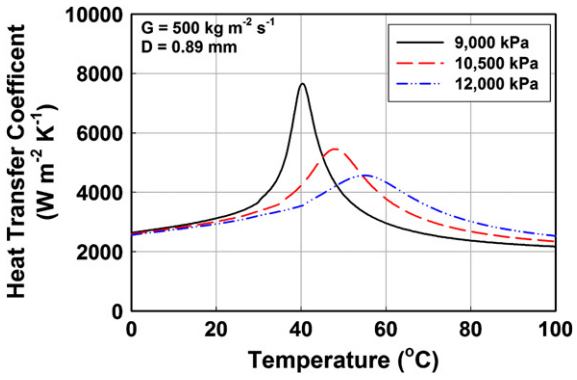

Fig. 7 – Refrigerant heat transfer coefficient vs. temperature.

temperature approaches the pseudo-critical temperature, the specific heat and other transport properties change drastically, yielding the spike in heat transfer coefficient. The temperature corresponding to the pseudo-critical temperature increases as the refrigerant pressure is increased. These effects are illustrated in Fig. 7, which shows a plot of CO_2 heat transfer coefficient at a mass flux of 500 kg m^{-2} s^{-1}, in a circular channel with ID = 0.89 mm, at three different pressures and temperatures ranging from 0 to 100 °C. The heat transfer coefficient is calculated using the Gnielinski (1976) correlation. As seen in Fig. 7, at a given pressure, the heat transfer coefficient spike is a function of the refrigerant temperature. Thus, as mass flow rate increases, the temperature change across the heat exchanger decreases and the spike shifts towards the refrigerant outlet. Further increasing the mass flow (and decreasing the temperature glide) would result in this spike not being observed, as the refrigerant would not cool into the pseudo-critical region.

For the water-coupled CO_2 gas cooler under consideration, the refrigerant-side resistance is generally the limiting factor. This is illustrated in Figs. 8 and 9. Fig. 8 shows the diminishing returns in overall UA with increasing water flow rate for refrigerant mass flow rates of 12 g s^{-1} and 24 g s^{-1}. The reported UA is the summation of the UA of each segment in the gas cooler model. The water flow rate is varied from 0.93 to 9.5 L min^{-1} at an inlet temperature of 5 °C. Increasing the water flow rate to 150% from 0.93 L min^{-1} to 2.38 L min^{-1} results in a 28% increase in UA for the 12 g s^{-1} mass flow rate, and 31% for the 24 g s^{-1} mass flow rate. However, increasing the water flow 66%, from 5.68 to 9.5 L min^{-1}, results in an increase in UA of only 1 and 4% for the 12 g s^{-1} and 24 g s^{-1} refrigerant flow rates, respectively. For a fixed water flow rate, doubling the refrigerant mass flow rate from 12 g s^{-1} to 24 g s^{-1} results in an increase in UA of 41, 58, 87 and 92% at flow rates of 0.93, 2.38, 5.68 and 9.5 L min^{-1} respectively. It can be seen that at water flow rates greater than 0.93 L min^{-1}, doubling the refrigerant mass flow rate results in large percentage increases in UA, whereas increasing the water flow rate has diminishing returns. This indicates that the refrigerant-side presents the limiting resistance in the heat transfer process.

Fig. 9 tracks the refrigerant-to-water thermal resistance ratio and refrigerant temperature through the gas cooler with a water flow rate of 0.93 L min^{-1} and 5 °C inlet temperature, and refrigerant flow rates of 12 g s^{-1} and 24 g s^{-1} at an inlet temperature of 100 °C and pressure of 9000 kPa. Refrigerant

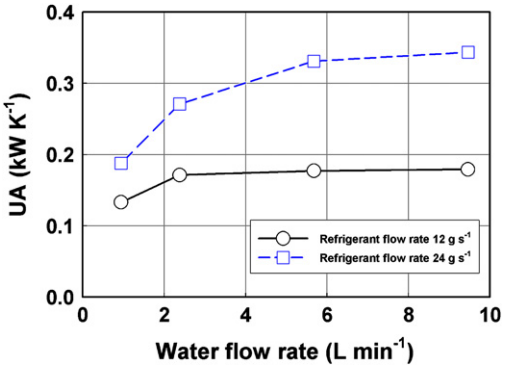

Fig. 8 – UA vs. water flow rate.

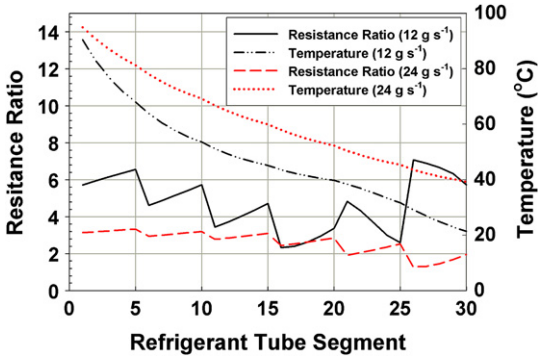

Fig. 9 – Refrigerant/water resistance ratio.

and water-side thermal resistances are defined as a function of heat transfer coefficient and effective heat transfer area as shown in Eqs. (9) and (10).

$$R_{ref} = \frac{1}{h_{ref} A_{ref}} \tag{9}$$

$$R_{water} = \frac{1}{h_{water} A_{water}} \tag{10}$$

Fig. 9 further confirms the conclusions from Fig. 8 that the refrigerant-side thermal resistance in general limits the heat transfer process for both mass flows examined. While Fig. 9 shows the resistance ratio at a water flow of 0.93 L min^{-1}, Fig. 8 shows that the ratio will only become increasingly limited by the refrigerant-side resistance as water flow rate increases. Thus, increasing the water flow rate would yield little improvement in heat transfer performance. For the 12 g s^{-1} refrigerant flow rate, a dip in refrigerant thermal resistance is observed when the refrigerant temperature is near the pseudo-critical temperature of 40 °C (segments 15–20). This is attributed to the spike in refrigerant heat transfer coefficient, resulting from the rapidly changing thermodynamic and transport properties. For the 24 g s^{-1} flow rate, the refrigerant temperature remains above the pseudo-critical temperature until near the outlet of the gas cooler, and the dip in thermal resistance ratio is not observed until this region (segments 25–30). These changes in resistances correspond to the increase in local heat duty observed in Fig. 6.

The implications of this observation are as follows: (1) if refrigerant temperature is not reduced below the pseudo-critical temperature, either due to an undersized heat exchanger or a high water inlet temperature, the enhanced heat transfer in the pseudo-critical region will not be realized; and (2) increasing refrigerant pressure generally raises the pseudo-critical temperature, which dampens the spike in refrigerant heat transfer coefficient as seen in Fig. 7, but expands the temperature range in which heat transfer is enhanced. Thus, CO_2 gas cooler performance will be sensitive to water inlet temperature, water flow rate and refrigerant inlet pressure, as shown in Figs. 10 and 11. Heat duty (Fig. 10) and the approach temperature difference (Fig. 11) are plotted as a function of water inlet temperature for a refrigerant inlet temperature of 100 °C, refrigerant mass flow rate of 16 g s^{-1}, refrigerant pressures of 9000, 10500 and 12,000 kPa, and water

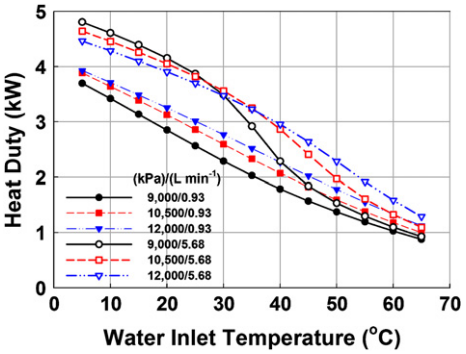

Fig. 10 – Heat duty vs. water inlet temperature.

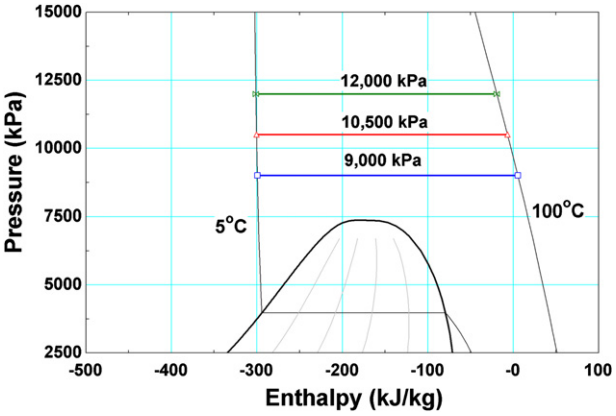

Fig. 12 – Carbon dioxide P–h diagram.

flow rates of 0.93 L min^{-1} and 5.68 L min^{-1}. Approach temperature difference is defined in Eq. (11).

$$\Delta T_{approach} = T_{ref,out} - T_{water,in} \quad (11)$$

With all other parameters fixed, the heat duty is seen to increase with increasing refrigerant inlet pressure for the 0.93 L min^{-1} flow rate case at each water inlet temperature. As was shown in Fig. 7, for these cases, as the refrigerant pressure increases, the temperature band corresponding to the improved heat transfer coefficient widens and shifts to a higher temperature. Thus, the improved local refrigerant-side heat transfer coefficient corresponds to a locally higher driving temperature difference for a longer portion of the CO_2 temperature glide. Examination of Fig. 11 for the 0.93 L min^{-1} case indicates that the seven-plate gas cooler is undersized for nearly all inlet refrigerant pressures and water inlet temperatures. An ideally sized gas cooler would have an approach temperature difference approaching zero. For the 0.93 L min^{-1} water flow rate, the approach temperature differences are as high as 27 K at a water inlet of 5 °C. As the water inlet temperature increases, the heat duty and the approach temperature both decrease. Since the refrigerant outlet can only be driven down to a temperature equal to the water inlet, the enthalpy difference between the refrigerant inlet and outlet decreases. This decrease is not a linear relationship, and varies dramatically near the pseudo-critical temperature and with pressure. As the water outlet temperature rises above this, the available refrigerant enthalpy difference decreases. The effect of this can be seen in the shape of the approach temperature difference curve for the 0.93 L min^{-1} water flow case at 9000 kPa.

Increasing the water flow rate to 5.68 L min^{-1} results in some different trends. Fig. 11 shows that for the higher water flow rate, approach temperature difference is low (<5 K) for all water inlet temperatures. In this case, with the refrigerant inlet temperature and mass flow rates fixed, the heat duty in Fig. 10 decreases with increasing pressure. As a comparison, in a conventional refrigerant system, increasing the high-side pressure will raise the saturation temperature while decreasing the enthalpy of vaporization. This allows higher water outlet temperature, but also reduces the maximum potential heat duty, with all other parameters fixed. For supercritical CO_2, the temperature and pressure can vary independently. Examination of a CO_2 P–h diagram (Fig. 12) shows that above the critical point, with the same refrigerant inlet and outlet temperatures, increasing the pressure will decrease the available enthalpy difference due to the shape of the isotherms. Thus, for a gas cooler designed in a manner that $T_{ref,out} \rightarrow T_{water,in}$, increasing the pressure while maintaining the same refrigerant inlet temperature will decrease heat duty, since the limiting factor is the available enthalpy difference. For a gas cooler with a large approach temperature difference, increasing the pressure at the same refrigerant inlet temperature will result in an increase in heat duty, as the extended temperature range of elevated specific heat is utilized, and the heat duty is not limited by the total available enthalpy difference.

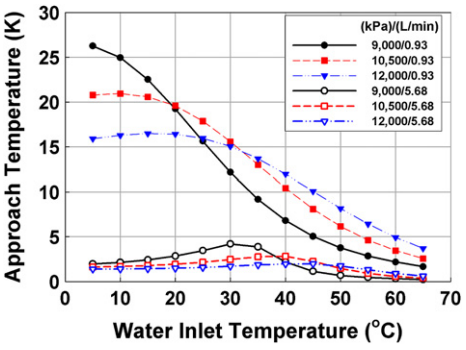

Fig. 11 – Approach temperature vs. water inlet temperature.

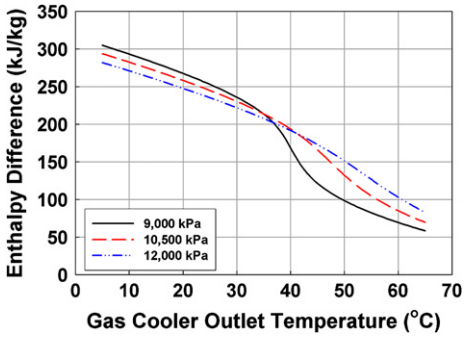

Fig. 13 – CO_2 Enthalpy difference vs. outlet temperature.

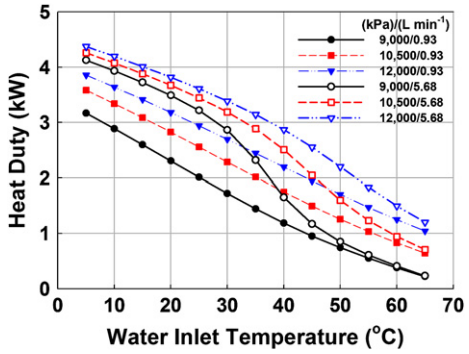

Fig. 14 – Heat duty vs. water inlet temperature (isentropic compression).

The inflection points observed in Fig. 10 for the 5.68 L min^{-1} water flow rate at 9000 kPa can be attributed to the same inherent CO_2 properties that caused the inflection points in the approach temperature difference curve discussed earlier. Fig. 13 shows a plot of CO_2 enthalpy difference assuming an inlet temperature of 100 °C, and an outlet from 5 to 65 °C at three different refrigerant pressures. This is a good approximation of the predicted gas cooler behavior observed in Fig. 10 for the 5.68 L min^{-1} water flow rate. In Fig. 13, at a refrigerant pressure of 9000 kPa, an inflection in the available enthalpy difference can be observed in the pseudo-critical regime. These inflections dampen out and shift to higher temperatures as pressure is increased. This illustrates the sensitivity of gas cooler design to water inlet temperature, particularly at lower refrigerant pressures and at temperatures around the critical temperature.

The information presented in Figs. 10–13 shows that for a given gas cooler with a fixed refrigerant inlet and mass flow rate, as approach temperature difference tends towards zero, increasing refrigerant pressure results in decreased heat duty and system COP. In reality, the refrigerant inlet temperature is a function of many variables including evaporator temperature, compressor efficiency, charge level and superheat. While supercritical CO_2 temperature and pressure are independent variables, in an actual system, increasing high-side pressure with a fixed compressor and evaporation temperature will generally result in an increased high-side temperature. This increases the driving temperature difference, and mitigates the decreasing enthalpy difference effects with fixed refrigerant and water inlet temperatures observed in Figs. 10 and 11. Assuming an evaporation temperature of 0 °C, isentropic compression and high-side pressures of 9000, 10,500 and 12,000 kPa, the corresponding refrigerant inlet temperatures are 72.5, 85.5, and 96.8 °C. Fig. 14 shows the model results using these refrigerant inlet temperatures and corresponding pressures, a fixed refrigerant mass flow rate of 16 g s^{-1}, water flow rate of 0.93 L min^{-1} and 5.68 L min^{-1} and water inlet temperature from 5 to 65 °C.

Assuming isentropic compression from a fixed evaporation temperature, with identical mass flow, increasing the pressure (and the corresponding inlet temperature) will result in an increase in heat duty, as seen in Fig. 14. With a refrigerant flow rate of 16 g s^{-1} and a water inlet temperature of 5 °C, increasing the pressure 33% results in an increased heat duty of 22% for a water flow of 0.93 L min^{-1} and 5.8% for 5.68 L min^{-1}. At a water temperature near the pseudo-critical regime (45 °C), an increase in pressure of 33% yields an increase in heat duty of 104% for the 0.93 L min^{-1} water and 117% for the 5.68 L min^{-1} water flow cases. In general, as discharge pressure and compression ratio increase, compressor volumetric efficiency and isentropic efficiency tend to decrease. Thus, in reality, designing a system with higher gas cooler refrigerant pressure may not be as beneficial as theoretically possible.

4. Conclusions

The results presented here show that accurate modeling of gas cooler performance is critical to designing an efficient transcritical CO_2-water heating system. In a water-coupled gas cooler, the predicted performance is much more sensitive to the refrigerant heat transfer coefficient, compared to air-coupled systems dominated by the air-side resistance. Additionally, performance is sensitive to water inlet temperature. Increasing the water inlet temperature not only decreases the driving temperature differential, but as the temperature crosses the pseudo-critical temperature at a given pressure, causes a sudden change in available enthalpy difference. This effect is more pronounced at pressures closer to the critical pressure.

Many CO_2 vapor compression system models in the literature show that for a given compressor and gas cooler size, there is an optimum high-side pressure at which COP is maximized. As shown in Figs. 10 and 11, this is true when the gas cooler is not designed in a manner in which approach temperature difference → 0. The analysis presented here shows that by sizing a CO_2 gas cooler in a segmented fashion, the approach temperature difference can be minimized, and the high-side system pressure can be reduced. An optimized compressor and system can then be designed and built around the gas cooler. The advantages of this are maximized COP for given operating conditions, a reduced pressure ratio, increased compressor efficiency and improved compressor reliability.

Commercial CO_2-water heating systems will need to rely on the high heat transfer coefficients, large heat transfer area-to-volume ratio, and ability to withstand high pressures that are characteristic of microchannels. The heat exchanger geometry modeled in this study offers better heat transfer performance with a smaller footprint than a tube-in-tube geometry.

While the present study has resulted in an accurate model for predicting the heat transfer performance of a water-coupled microchannel gas cooler, there are several areas in which additional work is needed:

- The model developed here should be incorporated into a water-coupled CO_2 vapor compression system model to predict the effects of changing water inlet temperature, high-side pressure, and evaporation temperature and compressor characteristics.
- The effect of compressor lubricant on supercritical carbon dioxide heat transfer coefficient during cooling in microchannels is not well understood. Investigations into this area may yield an even more accurate heat transfer model.

- Measurement of lubricant circulation rates in the test loop would provide a more accurate estimate of lubricant flow rates in the gas cooler, which would assist in more accurate computation of heat transfer coefficients and pressure drops.

Acknowledgments

The authors would like to acknowledge assistance from Mr. Christopher Goodman in design, fabrication, testing, analysis and modeling of the subject CO_2 components. Financial support from the US Army Ft. BelVoir office through a subcontract from Modine Manufacturing Company is also gratefully acknowledged. The authors also thank Modine Manufacturing Company for supplying several of the test heat exchangers and associated components. Assistance from, and insightful discussions with, Mr. John Manzione, Dr. Stephen B. Memory, Mr. David Garski, Mr. Sam Collier, and Mr. Mark Hoehne for conducting this research are also acknowledged.

REFERENCES

ASHRAE Standard, 2006. BRS/ASHRAE Standard 41.4-1996 (Ra 2006) Standard Method for Measurment of Proportion of Lubricant in Liquid Refrigerant. ASHRAE, Atlanta, GA.

Baskov, V.L., Kuraeva, I.V., Protopopov, V.S., 1977. Heat transfer with the turbulent flow of a liquid at supercritical pressure in tubes under cooling conditions. Teplofizika Vysokikh Temperatur 15 (1), 96–102.

Cecchinato, L., Corradi, M., Fornasieri, E., Zamboni, L., 2005. Carbon dioxide as refrigerant for tap water heat pumps: a comparison with the traditional solution. International Journal of Refrigeration 28 (8), 1250–1258.

Chang, Y.-S., Kim, M.S., 2007. Modeling and Performance Simulation of a Gas Cooler for a CO_2 Heat Pump System, vol. 13. HVAC&R Research, American Society of Heating, Refrigerating & Air-Conditioning Engineers, Inc., pp. 445–456.

Cheng, L., Ribatski, G., Thome, J.R., 2008. Analysis of supercritical co_2 cooling in macro- and micro-channels. International Journal of Refrigeration 31 (8), 1301–1316.

Churchill, S., 1977. Friction–factor equation spans all fluid flow regimes. Chemical Engineering 7, 91–92.

Dang, C., Hihara, E., 2004. In-tube cooling heat transfer of supercritical carbon dioxide. Part 1. Experimental measurement. International Journal of Refrigeration 27 (7), 736–747.

Filonenko, G.K., 1954. Hydraulic resistance of the pipelines. Thermal Engineering (4), 40–44.

Garimella, S., 2002. Microchannel gas coolers for carbon dioxide air-conditioning systems. ASHRAE Transactions 108 (1), 492–499.

Garimella, S., 2003. Conduction Effects in Cross-counterflow Supercritical Gas Coolers for Natural Refrigerants. International Congress of Refrigeration, Washington, DC.

Gnielinski, 1976. New Equations for heat and mass transfer in turbulent pipe and channel flow. International Chemical Engineering 16, 10.

Han, D.H., Lee, K.-J., 2005. Single-phase heat transfer and flow characteristics of micro-fin tubes. Applied Thermal Engineering 25 (11–12), 1657–1669.

Hoehne, M., 2007. Modine Manufacturing, Co.

Hwang, Y., Jin, D.-H., Radermacher, R., Hutchins, J.W., 2005. performance measurement of CO_2 heat exchangers. ASHRAE Transactions 111 (2), 306–316.

Kim, M.-H., Pettersen, J., Bullard, C.W., 2004. fundamental process and system design issues in CO_2 vapor compression systems. Progress in Energy and Combustion Science 30 (2), 119–174.

Kim, S.G., Kim, Y.J., Lee, G., Kim, M.S., 2005. The performance of a transcritical CO_2 cycle with an internal heat exchanger for hot water heating. International Journal of Refrigeration 28 (7), 1064–1072.

Klein, S.A., 2008. Engineering Equation Solver, F-Chart Software.

Koyama, S., Xue, J., Kuwahara, K., Takata, N., Yanagisawa, T., 2009. Simulation of a CO_2 transcritical cycle for air conditioning. 3rd IIR Conference on Thermophysical Properties and Transfer Processes of Refrigerants, Boulder, CO.

Krasnoshchekov, E.A., Kuraeva, I.V., Protopopov, V.S., 1970. Local heat transfer of carbon dioxide at supercritical pressure under cooling conditions. Teplofizika Vysokikh Temperatur 7 (5), 922–930.

Kuraeva, I.V., Protopopov, V.S., 1974. Mean friction coefficents for turbulent flow of a liquid at supercritical pressure in horizontal circular tubes. Teplofizika Vysokikh Temperatur 12 (1), 218–220.

Laipradit, P., Tiansuwan, J., Kiatsiriroat, T., Aye, L., 2008. Theoretical performance analysis of heat pump water heaters using carbon dioxide as refrigerant. International Journal of Energy Research 32 (4), 356–366.

Lockhart, R.W., Martinelli, R.C., 1949. Proposed correlation of data for isothermal two-phase, two-component flow in pipes. Chemical Engineering Progress 45, 39–48.

Manglik, R.M., Bergles, A.E., 1995. Heat transfer and pressure drop correlations for the rectangular offset strip fin compact heat exchanger. Experimental Thermal and Fluid Science 10 (2), 171–180.

Ortiz, T.M., Li, D., Groll, E.A., 2003. Evaluation of the Performance Potential of CO_2 as a Refrigerant in Air-to-air Air Conditioners and Heat Pumps: System Modeling and Analysis ARTI no. 21CR/610–10030.

Petrov, V.P., Popov, V.N., 1985. Heat transfer and resistance of carbon dioxide being cooled in the supercritical region. Thermal Engineering 32 (3), 131–134.

Pettersen, J., Hafner, A., Skaugen, G., Rekstad, H., 1998. Development of compact heat exchangers for CO_2 air-conditioning systems. International Journal of Refrigeration 21 (3), 180–193.

Pettersen, J., Rieberer, R., Munkejord, S.T., 2000. Heat Transfer and Pressure Drop for Flow of Supercritical CO_2 in Microchannel Tubes. SINTEF, Trondheim, Norway, TR, A5127 pp.

Petukhov, B.S., Kirillov, V.V., 1958. Heat exchange for turbulent flow of liquid in tubes. Teploenergetika 5 (4), 63–68.

Pitla, S.S., Groll, E.A., Ramadhyani, S., 2002. New correlation to predict the heat transfer coefficient during in-tube cooling of turbulent supercritical CO_2. International Journal of Refrigeration 25 (7), 887–895.

Pitla, S.S., Robinson, D.M., Groll, E.A., Ramadhyani, S., 1998. Heat transfer from supercritical carbon dioxide in tube flow: a critical review. HVAC&R Research 4 (3), 281–301.

Sarkar, J., Bhattacharyya, S., Gopal, M.R., 2006. Simulation of a transcritical CO_2 heat pump cycle for simultaneous cooling and heating applications. International Journal of Refrigeration 29 (5), 735–743.

Sarkar, J., Bhattacharyya, S., Ramgopal, M., 2009. A Transcritical CO_2 heat pump for simultaneous water cooling and heating: test results and model validation. International Journal of Energy Research 33 (1), 100–109.

Span, R., Wagner, W., 1996. A new equation of state for carbon dioxide covering the fluid region from the triple-point temperature to 1100 K at pressures up to 800 Mpa. Journal of Physical Chemistry 25 (6).

Wang, J., Hihara, E., 2002. Study on carbon dioxide gas cooler heat transfer process under supercritical pressures. International Journal of Energy Research 26 (14), 1237–1251.
White, F.M., 2003. Fluid Mechanics, fifth ed.. McGraw-Hill Higher Education, New York.
Yin, J.M., Bullard, C.W., Hrnjak, P.S., 2001. R-744 gas cooler model development and validation. International Journal of Refrigeration 24 (7), 692–701.
Zhao, Y., Ohadi, M.M., Radermacher, R., 2001. Micochannel Heat Exchangers with Carbon Dioxide ARTI no. 21CR/604-10020-01.